Direct Measurement of Transverse Coherence Length of Hard X Rays from Interference Fringes

V. Kohn,[1] I. Snigireva,[2] and A. Snigirev[2,*]

[1]*Russian Research Centre "Kurchatov Institute," 123182 Moscow, Russia*

[2]*European Synchrotron Radiation Facility, B.P. 220, F-38043, Grenoble Cedex, France*

(Received 17 November 1999)

We propose a simple interferometric technique for hard x-ray spatial coherence characterization, recording a Fresnel interference pattern produced by a round fiber or a slit. We have derived analytical formulas that give a direct relation between a visibility of interference fringes and either the source size or the transverse coherence length. The technique is well suited to third-generation synchrotron radiation sources and was experimentally applied to determine the spatial coherence length and the source size at the European Synchrotron Radiation Facility.

PACS numbers: 41.60.Ap, 41.50.+h, 42.25.Kb, 61.10.Dp

With an appearance of third generation synchrotron radiation sources such as ESRF, SPring 8, and APS, the field of coherent optics has expanded its borders into the domain of high energy x-ray radiation. When associating coherence with an ability to observe interference phenomena, we should distinguish between temporal coherence linked to the spectral bandwidth (monochromaticity) of the beam and spatial (transverse) coherence which is related to the source size. A high level of spatial coherence, the really unique feature of these new sources, results from a very small source size of about 30 μm and a large source-to-object distance (around 50–100 m).

Using such a laserlike beam, coherent imaging techniques such as phase contrast imaging, holography, and interferometry have recently been proposed [1–5] and are currently under intensive development. State of the art online detectors [6], together with optical elements created on diffraction and refraction principles [7–12], open real opportunities to overcome visible light limits and to go to submicrometer and even to nanometer resolution [9]. Under these new conditions the characterization and the manipulation of coherence are of great importance.

In the soft x-ray domain interferometry techniques were used for coherence measurements [13,14]. To measure a level of coherence in the field of hard x rays, optical elements such as crystals [15] or mirrors [16] were applied. However, as has been demonstrated, these optical elements can deteriorate transverse coherence and introduce additional errors in the true value of coherence level [17–21].

In this paper we propose a straightforward method for a spatial coherence characterization based on analyzing the visibility of Fresnel interference fringes produced by a well calibrated object like a fiber or a slit. Analytical formulas for a direct definition of the source size or the transverse coherence length have been derived for the first time. The proposed technique was experimentally applied to the source cross-section size characterization at the ESRF high-β undulator beam line ID 22. This beam line is well adapted for microimaging experiments with coherent x rays because the source size is small, a divergence is low, and an intensity is of order of 10^{12} photons/mm^2 at the sample position. A sketch of the experimental setup is schematically shown in Fig. 1. The energy of x rays selected by a silicon (111) monochromator was 10–20 keV. A transparent boron fiber and slits were located at the distance r_s from the source. Interference patterns were collected using an on-line detector with a 1 μm thick transparent YAG scintillator coupled by a light microscope to a CCD camera. A detector has a pixel size of 0.32 μm, and a FWHM of the point-spread function is equal approximately to 0.8 μm [6]. The detector was placed at the distance r_d from the object.

We assume that the synchrotron radiation source consists of very many incoherent point sources transversely distributed according to the Gaussian law. Each point source radiates an approximately spherical monochromatic wave. The fiber and the slit as linear objects disturb a wave front only along the x direction (see Fig. 1). As is known for in-line imaging geometry, each point source located at the position x_s produces an identical interference pattern on the detector, but shifted by the value $-x_s r_d/r_s$. Therefore the interference pattern calculated for the point source at the optical axis must be averaged over $w_s r_d/r_s$, where w_s is the source size.

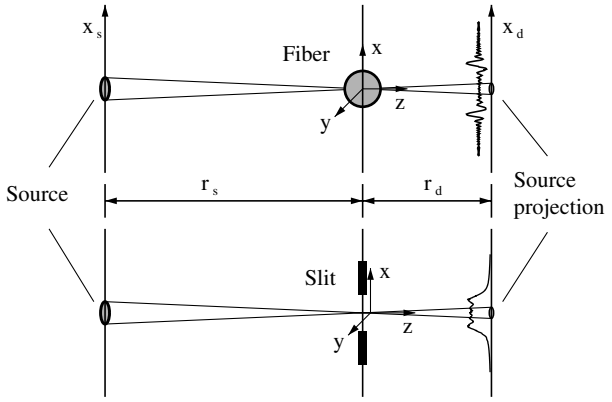

FIG. 1. Schematic drawing of the experimental setup, where r_s is the distance from the source to fiber or slit and r_d is the distance from the fiber or slit to the high resolution detector.

An intensity distribution on the detector plane (image of the object) with the point radiator at a center of the source $I_0(x_d) = |E(x_d)|^2$ is described by the Fresnel-Kirchhoff integral [22] applying a small angle approximation

$$E(x_d) = \frac{1}{\sqrt{r_t}} \int_{-\infty}^{\infty} dx\, P(x_d - x, r_d)\, F(x) S(x, r_s)\,, \tag{1}$$

where $S(x, r) = (1/\sqrt{r}) \exp(i\pi x^2/\lambda r)$ is a partial spherical wave along the x axis, λ is a wavelength, $P(x, r) = S(x, r)/\sqrt{i\lambda}$ is a propagator along the x axis, $r_t = r_s + r_d$ is a total distance source-to-detector, and we have omitted an unessential phase factor. The complex transmission amplitude $F(x)$ is determined by a size, a shape, and a structure of the object. In the case of the fiber of radius R it is equal to unity for $|x| > R$ and $\exp[-(4\pi/\lambda)(\beta + i\delta)\sqrt{R^2 - x^2}]$ for $|x| < R$, where δ is a decrement of refractive index, and β is an index of absorption. In the case of the slit we have $F(x) = \theta(a/2 - |x|)$ where $\theta(x)$ is the Heaviside step function and a is a slit width.

An intensity measured experimentally in the in-line imaging geometry is

$$I(x_d) = \int dx_s\, B(x_s) I_0(x_d + x_s r_d/r_s)\,, \tag{2}$$

where the function $B(x_s)$ describes the brightness distribution of the source. We assume the function $B(x_s)$ to be Gaussian $B(x_s) = (1/\rho_s\sqrt{\pi}) \exp(-x_s^2/\rho_s^2)$, where $\rho_s = w_s/2$.

A visibility of fringes $V(x_d)$ in the region near the point x_d may be introduced as follows:

$$V(x_d) = \frac{I_{\max}(x_d) - I_{\min}(x_d)}{I_{\max}(x_d) + I_{\min}(x_d)}\,, \tag{3}$$

where $I_{\max}(x_d)$ and $I_{\min}(x_d)$ are the intensities corresponding to the maximum and adjacent minimum in the fringe system at the pointx_d.

The formulas presented above are well known (see, for example, [22]). These allow one to calculate the interference pattern and the visibility directly by means of computer simulations. Nevertheless, it is very useful to obtain approximate analytical expressions for the visibility which allow one to make a direct estimation of the transverse coherence length $l_{\rm tc}$ and the source size w_s. Below we present the formulas which were obtained by us for the first time. The method of derivation is described only shortly. The detailed analysis will be done later in a more extended article.

Fiber.—In the case of transparent fiber such a formula may be obtained by the use of the stationary phase approximation for calculating the integral (1). As known, the formulas obtained within this technique coincide with the results obtained employing an approximation of ray geometrical optics. The interference fringes arise due to interference between a direct ray coming from the source and a ray scattered by the object. However, near an edge of the fiber (the most important region) the standard stationary phase method [23] cannot be used due to the fact that the phase profile is not a slow varying function. We have developed the enhanced stationary phase method for calculating such a case. It takes into account the finite limits of integrating near the object edge. This leads to damping the intensity for the rays deviated in the vicinity of the edge.

As a result, we have obtained an analytical formula for the intensity distribution and the visibility of the fringes. The latter may be written in the region $x_d > 1.5R_d$ as follows:

$$V(x_d) = V_0(x_d) \exp\!\left(-\frac{(x_d - R_d)^2}{2s^2 l_{\rm tc}^2}\right), \qquad l_{\rm tc} = \frac{\sqrt{2}}{\pi}\,\frac{\lambda r_s}{w_s}\,, \tag{4}$$

where an exponential is directly related to the mutual coherence function (see, for example, [24]), $l_{\rm tc}$ is the transverse coherence length, $R_d = Rs$, and $s = r_t/r_s$ is a scaling factor. The function $V_0(x_d)$ is the visibility of the fringes for the case of point source

$$V_0(x_d) = \frac{2A(x_d)}{1 + A^2(x_d)}\,, \tag{5}$$

where

$$A(x_d) = \frac{g(x_d) f^{1/2}(x_d)}{[1 + f(x_d)]^{1/2}}, \qquad f(x_d) = \frac{(2\delta r_d)^2 R_d}{(x_d - R_d)^3}\,. \tag{6}$$

The other region outside fiber shadow where $x_d < -1.5R$ is symmetrical. The function $g(x_d)$ is obtained from the enhanced stationary phase technique, and it cannot be represented by simple formula. However, it can be shown that $g(x_d)$ has values between 1 (for fringes near the fiber shadow edge) and 0.5 (for far fringes).

The experiment was done with the boron fiber of 50 μm radius having a 15 μm tungsten core for the following experimental conditions: $r_s = 41$ m, $r_d = 5$ m, and x-ray energy $\hbar\omega = 17$ keV. Figure 2(a) shows the experimentally measured intensity distribution in arbitrary units. A number of well pronounced interference fringes was observed outside the fiber shadow. Measuring the visibility of the fringes in the region $|x_d| > 1.5R_d$ we obtain the source size $w_s = (33 \pm 4)$ μm using the formula

$$w_s = \frac{2}{\pi}\,\frac{\lambda r_t}{(|x_d| - R_d)}\,\ln^{1/2}\!\left(\frac{V_0(|x_d|)}{V(|x_d|)}\right), \tag{7}$$

where $V_0(|x_d|)$ was calculated with $g(|x_d|) = 0.75$. The transverse coherence length $l_{\rm tc} = (41 \pm 5)$ μm is calculated from the formula (4). The result of computer simulation of the intensity distribution for this case is shown in Fig. 2(b) for a point source and Fig. 2(c) for a source of 33 μm size. One may see that the calculated intensity profile [Fig. 2(c)] reproduces approximately the experimental pattern [Fig. 2(a)]. A contrast and a distance between the

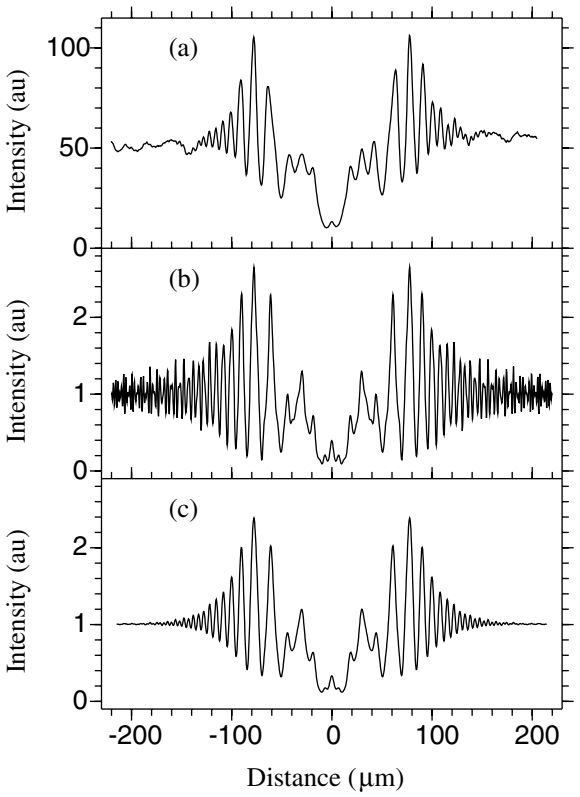

FIG. 2. Diffraction fringes produced by the boron fiber of 100 μm diameter with a 15 μm tungsten core. Fiber is placed at 41 m from the source; the distance fiber-to-detector is 5 m; the x-ray energy is 17 keV. (a) The experimental data, (b) theoretical calculation for a point source, and (c) theoretical calculation for a 33 μm source size.

fringes coincide closely. However, the experimental pattern contains some extra perturbations of the fringes caused by imperfections of the optical elements in the beam path, in particular, vacuum windows, filters, and monochromator crystals [17–19].

Slit.—The light diffraction by a slit is a classical optical example. As known, when a wave passes through a slit of a width a, a transition from Fresnel to Fraunhofer diffraction can be observed. A distance dividing the two regimes is known as a Rayleigh distance and is given by a^2/λ. The accurate theoretical intensity distribution is described by Fresnel integrals. To obtain an analytical approximate expression we used an asymptotic behavior of Fresnel integrals [25] which is valid for a central part of a slit shadow. We find that a visibility of the central fringe is determined as

$$V = V_0 \exp(-\rho^2/2l_{\mathrm{tc}}^2), \tag{8}$$

where $\rho = a/2$ and the transverse coherent length l_{tc} is defined by (4). The visibility of the central fringe in the case of point source is described by

$$V_0 = \frac{4}{\pi}\frac{a_0}{a}\left|\cos\left[\pi\left(\frac{a^2}{a_0^2} - \frac{3}{4}\right)\right]\right|, \tag{9}$$

where $a_0^2 = 4\lambda r_d r_s/r_t$, and $r_t = r_s + r_d$. This formula is valid when $a > a_0$.

We have done an experiment with $r_s = 31$ m, $r_d = 10$ m, $\hbar\omega = 18$ keV. Diffraction images of the slits of different sizes were registered. Figure 3(a) shows experimental results for the slit of 100 μm size, where the visibility value $V = 0.11 \pm 0.01$ was measured for the central fringe. Then the formulas (8) and (9) give the following estimation of source size $w_s = 27.2\ \ln^{1/2}(0.58/V)$ μm. With the measured V value we obtain $w_s = (35 \pm 3)$ μm that correlates with the above estimation by means of fiber. The transverse coherence length is $l_{\mathrm{tc}} = (27 \pm 2)$ μm in this case. The calculated diffraction pattern in the case of the point source and the condition specified above is shown in Fig. 3(b); the pattern after a smoothing over the source size of 35 μm is shown in Fig. 3(c). As may be inferred from Fig. 3 the measured interference pattern is reproduced within the approximation limits by calculated intensity distribution for 35 μm source size.

Summary.—We proposed and tested a new technique of measuring the source size on third-generation synchrotron radiation sources by means of in-line imaging of the objects with a known structure such as a fiber or a slit. We have derived the analytical formulas which allow us to estimate directly the source size and the transverse coherence

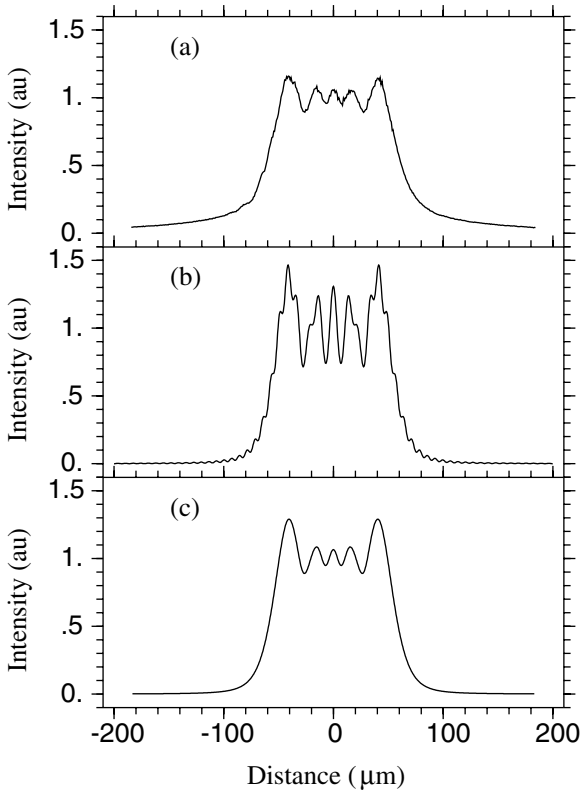

FIG. 3. Fresnel diffraction on the 100 μm slit. Slit is located on 31 m from the source; distance slit-to-detector is 10 m, the energy of x rays is 18 keV. (a) The experimental pattern, (b) theoretical calculation for a point source, and (c) theoretical calculation for a 35 μm source size.

length of the beam. The analytical results are verified by computer simulation technique. At the ID 22 beam line we measured the source size of 35 μm, which is in accordance with the data provided by the ESRF machine group at the time of the experiment. The advantage of the proposed technique is that it keeps instrumental errors to the minimum. This technique also allows one to characterize the influence on coherence by optical elements implemented in the experimental setup. In view of the development of x-ray free-electron lasers (1 Å wavelength), this technique appears to be very promising and of particular value.

*Email address: snigirev@esrf.fr

[1] A. Snigirev, I. Snigireva, V. Kohn, S. Kuznetsov, and I. Schelokov, Rev. Sci. Instrum. **66**, 5486–5492 (1995).
[2] C. Raven, A. Snigirev, I. Snigireva, P. Spanne, A. Souvorov, and V. Kohn, Appl. Phys. Lett. **69**, 1826–1828 (1996).
[3] Z. H. Hu, P. A. Thomas, A. Snigirev, I. Snigireva, A. Souvorov, P. G. R. Smith, G. W. Ross, and S. Teat, Nature (London) **392**, 690–693 (1998).
[4] P. Spanne, C. Raven, I. Snigireva, and A. Snigirev, Phys. Med. Biol. **44**, 741–749 (1999).
[5] T. E. Gureyev, C. Raven, A. Snigirev, I. Snigireva, and S. W. Wilkins, J. Phys. D **32**, 563–567 (1999).
[6] A. Koch, C. Raven, P. Spanne, and A. Snigirev, J. Opt. Soc. Am. **15**, 1940–1951 (1998).
[7] A. Snigirev, Rev. Sci. Instrum. **66**, 2053–2058 (1995).
[8] I. Snigireva, A. Souvorov, and A. Snigirev, in *X-ray Microscopy and Spectroscopy,* edited by J. Thieme, G. Schmahl, D. Rudolph, and E. Umbach (Springer-Verlag, Berlin, Heidelberg, 1998), Sec. IV37–IV44.
[9] W. Yun, B. Lai, Z. Cai, J. Masser, D. Legnini, E. Gluskin, Z. Chen, A. Krasnoperova, Y. Vladimirsky, F. Cerrina, E. Di Fabrizio, and M. Gentili, Rev. Sci. Instrum. **70**, 2238–2241 (1999).
[10] W. Yun, B. Lai, A. A. Krasnoperova, E. De Fabrizio, Z. Cai, F. Zerrina, Z. Chen, M. Gentilli, and E. Gluskin, Rev. Sci. Instrum. **70**, 3537–3541 (1999).
[11] A. Snigirev, V. Kohn, I. Snigireva, and B. Lengeler, Nature (London) **384**, 49–51 (1996).
[12] B. Lengeler, C. Schroer, M. Richwin, J. Tummler, M. Drakopoulos, A. Snigirev, and I. Snigireva, Appl. Phys. Lett. **74**, 3924–3926 (1999).
[13] Y. Takayama, R. Z. Tai, T. Hatano, T. Miyahara, W. Okamoto, and Y. Kagoshima, J. Synchrotron Radiat. **5**, 456–458 (1998).
[14] Y. Takayama, T. Hatano, T. Miyahara, and W. Okamoto, J. Synchrotron Radiat. **5**, 1187–1194 (1998).
[15] T. Ishikawa, Acta Crystallogr. A **44**, 496–499 (1988).
[16] K. Fezzaa, F. Comin, S. Marchesini, R. Coisson, and M. Belakhovsky, J. X-Ray Sci. Technol. **7**, 12–23 (1997).
[17] A. Snigirev, Proc. SPIE Int. Soc. Opt. Eng. **2856**, 26–33 (1996).
[18] A. Snigirev, I. Snigireva, V. Kohn, and S. Kuznetsov, Nucl. Instrum. Methods Phys. Res., Sect. A **370**, 634–640 (1996).
[19] I. Schelokov, O. Hignette, C. Raven, A. Snigirev, I. Snigireva, and A. Souvorov, Proc. SPIE Int. Soc. Opt. Eng. **2805**, 282–292 (1996).
[20] A. Souvorov, I. Snigireva, and A. Snigirev, Proc. SPIE Int. Soc. Opt. Eng. **3113**, 476–483 (1997).
[21] A. Souvorov, M. Drakopoulos, I. Snigireva, and A. Snigirev, J. Phys. D **32**, A184–A192 (1999).
[22] J. Cowley, *Diffraction Physics* (North-Holland, Amsterdam, 1975).
[23] H. Jeffreys and B. Swirles, *Method of Mathematical Physics* (Cambridge University Press, Cambridge, U.K., 1966).
[24] S. K. Sinha, M. Tolan, and A. Gibaud, Phys. Rev. B **57**, 2740–2758 (1998).
[25] *Handbook of Mathematical Functions,* edited by M. Abramowitz and I. A. Stegun, Applied Mathematic Series Vol. 55 (National Bureau of Standards, Washington, D.C., 1964).